第 29 卷 第 11 期 催 化 学 报 2008 年 11 月
Vol. 29 No. 11 Chinese Journal of Catalysis November 2008

文章编号: 0253-9837(2008)11-1178-09 综述: 1178～1186

乙烯基乙酸酯合成钯-金催化剂中金的助催化作用

陈明树[1], D. W. GOODMAN[2]
(1 厦门大学化学化工学院化学系和固体表面物理化学国家重点实验室, 福建厦门 361005;
2 德克萨斯 A &M 大学化学系, 德克萨斯州科利奇站, TX 77842-3012, 美国)

摘要: 硅胶负载的钯-金双金属催化剂是乙烯乙酰氧基化制乙烯基乙酸酯(VA)的高选择性催化剂,本文应用平面和负载纳米颗粒模型催化剂体系研究金的助催化作用,应用低能离子散射谱、低能电子衍射、X 射线光电子能谱、反射红外吸收光谱及程序升温脱附等技术表征这些模型催化剂. 结果表明,金的主要助催化作用是隔离催化剂表面的催化活性钯原子,形成孤立的钯活性中心,从而大大抑制或消除反应物和/或产物在毗邻多原子钯中心上的深度分解,提高 VA 合成的选择性及活性. 同时由于形成了孤立的钯原子活性中心,反应副产物或中间物之一的一氧化碳吸附较弱,避免了催化剂表面的一氧化碳中毒,进而提高催化活性.

关键词: 乙烯基乙酸酯; 双金属; 钯; 金; 合金效应
中图分类号: O643 **文献标识码**: A

Promotional Effects of Au in Pd-Au Catalysts for Vinyl Acetate Synthesis

CHEN Mingshu[1], D. W. GOODMAN[2 *]
(1 State Key Laboratory of Physical Chemistry of Solid Surfaces, Department of Chemistry, College of Chemistry and Chemical Engineering, Xiamen University, Xiamen 361005, Fujian, China; 2 Department of Chemistry, Texas A &M University, College Station, TX 77842-3012, USA)

Abstract: Silica supported Pd-Au bimetallic catalysts are highly selective for the acetoxylation of ethylene to vinyl acetate (VA). In this study we have used model catalysts consisting of planer surfaces and supported nanoparticles to investigate the promotional effects of Au in Pd-Au bimetallic catalysts. Low energy ion scattering spectroscopy, low energy electron diffraction, X-ray photoelectron spectroscopy, infrared reflection adsorption spectroscopy, and temperature-programmed desorption et al, were used to characterize the model systems. The catalytic performance for acetoxylation of ethylene to VA was examined for these model surfaces. In this paper, we summarize the current understanding of the promotional effects of Au in Pd-Au bimetallic catalysts for VA synthesis. The key results are that Au atoms break contiguous Pd atom ensembles at the surface into isolated Pd monomers. The absence of contiguous Pd sites significantly reduces the formation of combustion by-products and suppresses the poison effects of CO, thus enhancing the VA formation selectivity and activity.

Key words: vinyl acetate; bimetal; palladium; gold; alloy effect

Bimetallic alloy systems are important in numerous technological applications, including metallurgy, catalysis, electrochemistry, magnetic materials, and microelectronics fabrication[1,2]. In heterogeneous catalysis, for example, the addition of a second metal component can greatly enhance the catalytic performance, particularly with respect to activity and selectivity[2-5]. A thorough understanding of the reaction mechanism over bimetallic surfaces at the atomic level can aid in understanding reaction mechanisms and in the optimization of catalytic performance.

The Pd-Au system is one of the most extensively

Received date: 22 September 2008.
* **Corresponding author.** Tel: +1-979-845-0214; Fax: +1-979-845-6822; E-mail: goodman@mail.chem.tamu.edu
Foundation items: Supported by Department of Energy, Office of Basic Energy, Division of Chemical Sciences, and Robert A. Welch Foundation.
English edition available online at ScienceDirect (http://www.sciencedirect.com/science/journal/18722067).

studied and utilized bimetallic heterogeneous catalyst[2,3,6-23]. Pd is an active catalyst for the acetoxylation of ethylene to vinyl acetate (VA), see equation (1)[2,3,24-36]. However Pd is also an active catalyst for the combustion of ethylene and acetic acid and thus exhibits a low selectivity for VA synthesis (Equations (2) and (3)).

$$CH_3COOH + C_2H_4 + O_2 \longrightarrow CH_3COOCHCH_2 + H_2O \quad (1)$$

$$CH_3COOH + O_2 \longrightarrow CO_2(+CO) + H_2O \quad (2)$$

$$C_2H_4 + O_2 \longrightarrow CO_2(+CO) + H_2O \quad (3)$$

The addition of small amounts of Au to a supported Pd catalysts can significantly enhance its selectivity and activity for this reaction, as shown in Fig 1[2,3,28-31]. Silica supported Pd-Au bimetallic catalysts promoted with potassium acetate have been used as commercial catalysts for VA synthesis for more than 40 years. However, the overall reaction mechanism and the promotional effect of Au are still unclear. In this study, we have used model catalyst surfaces combined with modern surface science techniques to investigate the promotional effect of Au in Pd-Au catalysts.

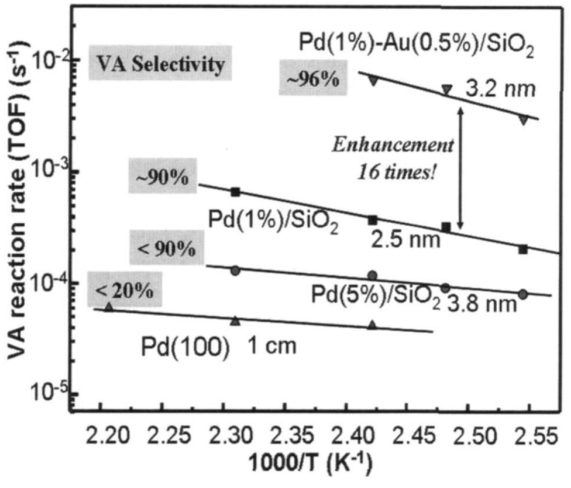

Fig 1　Vinyl acetate (VA) formation rates (TOF) as a function of reaction temperature on various Pd based catalysts

(Reaction conditions: acetic acid, ethylene, and O_2 partial pressures are 8.33×10^2, 1.07×10^3, and 2.66×10^3 Pa, respectively, with He as balance gas.)

1　Experimental

The experiments were carried out in several ultrahigh vacuum (UHV) chambers equipped with X-ray photoelectron spectroscopy/low energy ion scattering spectroscopy (XPS/LEIS), high resolution electron energy loss spectroscopy (HREELS), infrared reflection adsorption spectroscopy (IRAS) or XPS/reactor. Each chamber was also equipped with basic surface science techniques of low energy electron diffraction (LEED), atomic emission spectrometry (AES), and temperature-programmed desorption (TPD). The base operating pressures was $\sim2.66\times10^{-8}$ Pa. The XPS and LEIS spectra were collected using a concentric hemispherical analyzer (PHI, SCA 10-360) using Ne^+ ions at 0.75 keV and an ion beam scattering angle of $\sim45^\circ$ with respect to the surface normal. A Mattson Cygnus 100 FT-IR spectrometer was used for the IRAS measurements. The IR spectra were acquired using 4 cm^{-1} resolution and 512 scans in the single reflection mode at an incident angle of 84° with respect to the surface normal. The Mo(110) single crystal was mounted by a Ta wire on a transferable probe capable of liquid nitrogen cooling to 80 K and resistive heating to 1 500 K or by e-beam heating to 2 400 K. The sample temperature was monitored with a W-5% Re/W-26% Re (type C) thermocouple which was spot-welded to the back of the Mo(112) single crystal. The TPD apparatus utilizes a line-of-sight quadruple mass spectroscopy (QMS) with a differentially pumped aperture and a linear heating ramp of 5 K/s. These experimental systems have been described in detail elsewhere[3,34,35].

The Mo(112) single crystal was cleaned by oxidation (1 200 K, 6.67×10^{-5} Pa O_2) and vacuum annealing (2 200 K) cycles until no carbon and oxygen was detected by AES and a sharp (1×1) LEED pattern was observed. Pd and Au were evaporated from dosers made of high-purity Pd and Au wires (99.99%) wrapped around Ta filaments. Impurities were removed by thoroughly degassing before dosing. All the metal depositions were performed with the sample at room temperature. The dosing rates were calibrated by LEIS, XPS, or AES breaking point. One monolayer (ML) is defined as one Pd (or Au) atom per substrate surface atom. Carbon monoxide and oxygen (99.99%, Matheson Gas Products) were further purified by fractional condensation, then transferred to glass bulbs attached to the chamber gas manifold. High purity deuterated ethylene (99%, Aldrich) was used without further purification. The silicon doser consisted of a high-purity silicon sliver wrapped with a W-wire and resistively heated. The details of the SiO_2 film preparation have been described previously[37,38].

The VA synthesis experiments were carried out

in a combined elevated-pressure reactor-UHV XPS chamber[3,39]. After preparation and characterization in the UHV chamber, the Pd/Au(100) sample was transferred in-vacuo into the reaction chamber through a double-stage, differentially pumped Teflon sliding seal. Glacial acetic acid (CH_3COOH) was further purified by triple distillation; research-grade ethylene (C_2H_4) and ultra-high purity O_2 were used as received. A CH_3COOH :C_2H_4 :O_2 (2 :4 :1) mixture with a total pressure of 1.87×10^3 Pa was used for the kinetic studies. The VA product was analyzed by gas chromatography (GC) using a flame ionization detector (FID).

2 Results and discussion

2.1 Catalytic performance for VA synthesis on model surfaces

VA synthesis was carried out at 453 K on model surfaces of both Pd/Au(100) and Pd/Au(111), respectively[3]. Pd atoms were evaporated onto clean Au(100) or Au(111) surfaces from a filament source followed by an anneal at 550 K for 10 min. The samples were then in-vacuo transferred into the reaction cell. 8.33×10^2 Pa of acetic acid was first introduced into the reaction cell, then 1.33×10^3 Pa of an ethylene and O_2 mixture (4 :1) was added. The sample was heated to 453 K and held at this temperature for 3 h. The reaction products were analyzed using GC. The rate of VA formation is expressed as a turnover frequency (TOF), or the number of VA molecules produced per surface active site per second. Because the VA formation rate on Au(100) or Au(111) is negligible compared to the rate on Pd/Au or Pd surface, the catalytic active site is assumed to be surface Pd atoms. Therefore, the VA formation rate is computed based on the initial Pd coverage by assuming that all Pd atoms deposited remain on the surface during reaction. Plots of the VA formation rate (TOF) for Pd/Au surfaces as a function of the deposited Pd coverage are shown in Fig 2. The rate on the Au(100) surface increases significantly with a decrease in the Pd coverage, until a maximum is reached at a Pd coverage of ~0.07 monolayers. The corresponding VA formation rates for Pd on Au(111) rise steadily as the Pd coverage is decreased while, at all Pd coverages, the rates on Au(111) are significantly lower compared to the rate for the corresponding Pd coverage on Au(100), which reveals a structure-sensitive reaction[3]. The higher VA formation rates observed at relatively low Pd coverages demonstrate that

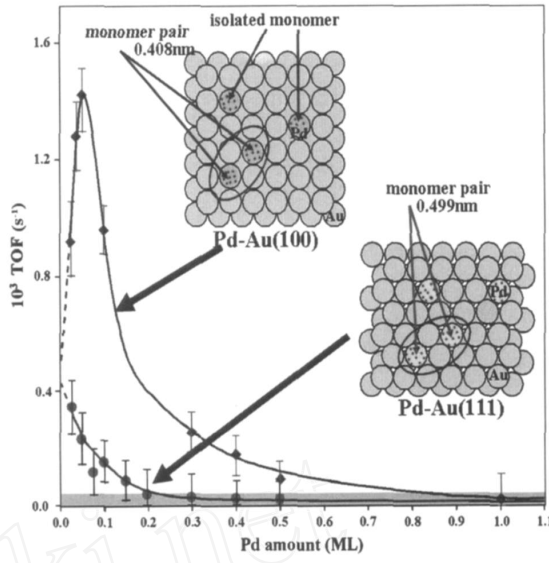

Fig 2 VA formation rates as a function of Pd coverage on Au(100) and Au(111)[3]

(The error bars are based on background rate data. The two inserts show Pd monomers and monomer pairs on the Au(100) and Au(111) surfaces. Reaction conditions: the VA synthesis was carried out at 453 K, with acetic acid, ethylene, and O_2 pressures of 5.33×10^2, 1.07×10^3, and 2.66×10^2 Pa, respectively. The total reaction time was 3 h.)

Pd sites, isolated by Au atoms, i.e, Pd monomers (shown in the schematic insert of Fig 2), are more active for VA synthesis than the surface ensembles containing contiguous Pd atoms. It is obvious that the relative amount of isolated Pd atoms is higher at lower Pd coverages, while that of contiguous Pd sites is higher at higher Pd coverages. In a recent report of electrocatalytic evolution of H_2 on a Au-Pd/Ru(0001) model surface, Pd monomers were found to be 20 times more active than contiguous Pd[13].

2.2 Surface Pd monomers

The formation of surface Pd monomers for Pd/Au(100) and Pd/Au(111) was probed by adsorption of CO using IRAS[3]. As shown in Fig 3(a), CO prefers to bond at the two-fold bridging and three-fold hollow sites on Pd(100) and Pd(111) surfaces, respectively[40-42]. Note that at saturation coverage of CO on Pd(111), a condensed phase forms with CO adsorbed at three-fold and atop sites. Intense CO vibrational features between 1 900 to 2 000 cm^{-1} corresponding to CO adsorption on two-fold bridging and/or three-fold hollow sites were observed for multilayer Pd on Au(100) and Au(111) deposited at or below room temperature (Fig 3 (b)). These data indicate formation of Pd overlayers on Au(111) or Au(100),

in agreement with previous studies[43,44]. After annealing Pd/Au(100) or Pd/Au(111) at 600 K, the CO features in the IRAS data corresponding to bridging and/or three-fold hollow sites disappear and the intensity of the features corresponding to atop sites between 2 080 to 2 125 cm^{-1} increase significantly. We emphasized that CO was adsorbed to saturation coverage at 100 K. These data demonstrate that surface alloying occurs upon annealing, and that contiguous Pd ensembles are eliminated leaving exclusively isolated Pd sites or monomers, i.e. Au_4Pd on Au(100) and Au_6Pd on Au(111) (see the schematic in Fig 2). The formation of surface Pd monomers has been observed by scanning tunneling microscopy (STM) on Au(111)[45] and Pd/Au(100) alloy[46].

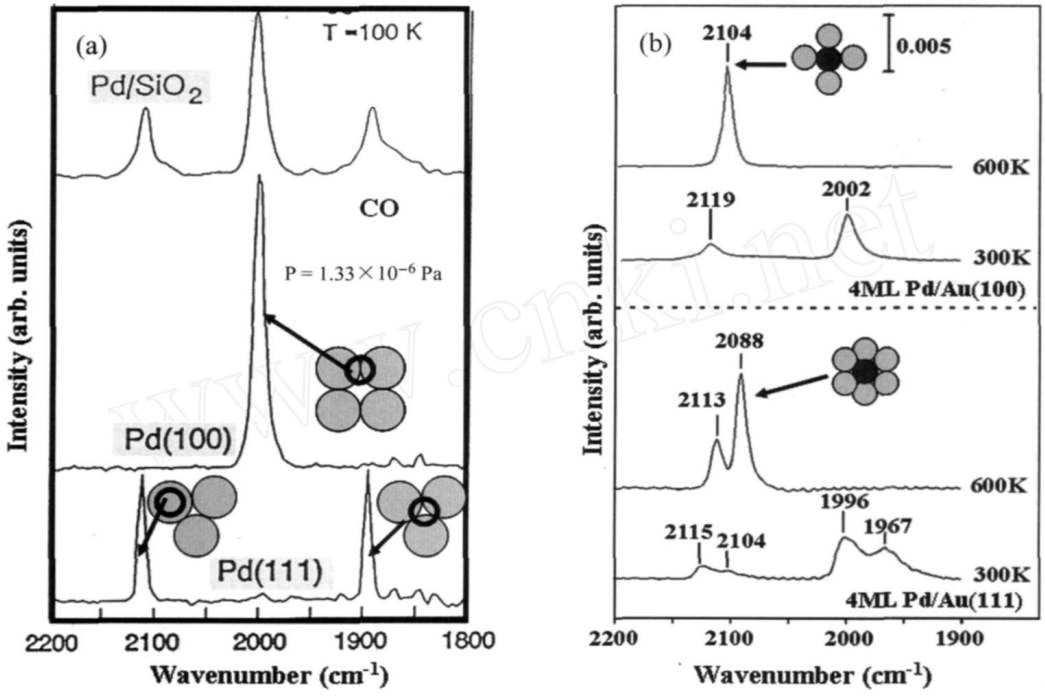

Fig 3　IRAS spectra for CO adsorption on: (a) Pd(111), Pd(100) and Pd nanoparticles with saturate coverage; (b) on Pd/Au(100) and Pd/Au(111) surfaces at 100 K showing the presence (300 K anneal) and absence (600 K anneal) of contiguous Pd sites[3]
(The Pd/Au(100) and Pd/Au(111) surfaces were prepared by depositing 4 ML of Pd at 100 K, then annealing to 300 and 600 K, respectively, for 10 min. The annealing temperatures are indicated on each spectrum.)

Alloying of Pd overlayers on a Au surface has also been observed for Pd/Au(111) after annealing at 500 K by LEIS, in which a significant decrease of surface Pd is evidenced[43]. We have used model planer surface alloys, Pd-Au/Mo(110), to examine the alloying between Pd and Au and the specific surface ensembles that form, see Fig 4[35]. Fig 4(a) shows LEIS spectra of 5 ML Pd/5 ML Au/Mo(110) as a function of annealing temperature. Following deposition of 5 ML Au onto Mo(110) at 300 K, only one LEIS feature at a relative energy of 0.97 was observed, while no substrate Mo feature at 0.89 is apparent. These results indicate that Au completely covers the Mo substrate at 5 ML Au. After deposition of 5 ML Pd on Au/Mo(110) surface, the Pd LEIS feature at 0.92 appears whereas the Au feature is significantly reduced but still detectable. The appearance of Au atoms at the surface can be attributed to interdiffusion between Pd/Au even at room temperature[43]. Upon annealing to 600 K, the Pd peak intensity gradually decreases with a corresponding increase in the Au peak intensity. With further annealing up to 1 000 K, the Au and Pd LEIS peak intensities change very little. Finally, the Au and Pd LEIS features disappear at around 1 200 and 1 300 K, respectively, due to desorption of Au and Pd. This is consistent with the appearance of Mo features at 0.89 after an anneal at 1 300 K. Fig 4(b) summaries the surface concentrations of Pd and Au as a function of annealing temperature. For a 5 ML Pd/5 ML Au surface, the surface concentration of Au gradually increases from 4 % to 80 % with an increase in the anneal temperature to 700 K, and then remains constant to 1 000 K. Above 1 000 K, the Au surface concen-

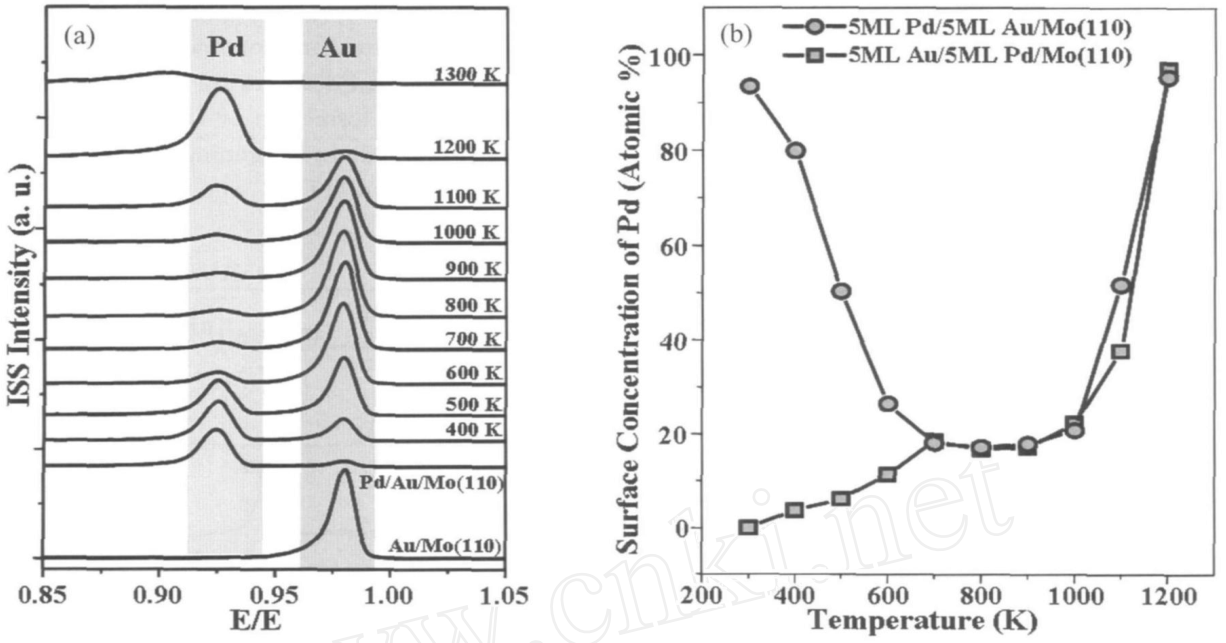

Fig 4 (a) LEIS spectra of 5 ML Pd/5 ML Au/Mo(110) as a function of annealing temperature. LEIS spectra were collected at 300 K after the sample was annealed to the specified temperature[35]. (b) Surface concentration of Au and Pd of 5 ML Pd/5 ML Au/Mo (110) and 5 ML Au/5 ML Pd/Mo(110) as a function of annealing temperature. The sample was annealed at each temperature for 20 min[35]

tration abruptly decreases because of Au desorption after which Pd dominates the surface. For 5 ML Au/5 ML Pd/Mo (110), the Pd surface concentration gradually increases from 0 to 20 % up to 700 K, then remains stable to 1 000 K. It is obvious that independent of the order of deposition, 5 ML Pd and 5 ML Au mixtures form a stable surface alloy between 700 and 1 000 K, with a surface consisting of ~20 % Pd and ~80 % Au. These results reflect the related lower surface free energy of Au vs Pd, e. g. Au (1.626 J/m^2)[47] vs Pd (2.043 J/m^2)[48] and also the alloying tendency between Pd and Au. The segregation of Au at the surface was also observed in the Au/Pd (111) system[49] and confirmed by theoretical calculation[50,51].

Similar with Pd/Au(100) and Pd/Au(111), CO was used as a probe molecule combined with IRAS to determine the surface ensembles of Pd-Au/Mo(110) as shown in Fig 5. Fig 5(a) shows IRAS spectra as a function of CO exposure at 90 K onto a 5 ML Pd/5 ML Au surface annealed at 600 K for 20 min. Two stretching features at 2 087 and 1 940 cm^{-1}, corresponding to CO at atop and bridged sites of Pd atoms, were observed for low CO exposure (< 0.10 L)[35,52,53]. With further CO exposure (≥0.20 L) a new feature appears at 2 105 cm^{-1} and is assigned to CO on atop sites of Au. Fig 5(b) shows IRAS spectra acquired at 90 K for CO adsorbed on a 5 ML Pd/5 ML Au surface annealed at 800 K for 20 min. Only a feature at 2 087 cm^{-1} appears within the low coverage CO regime (< 0.10 L), and a second feature at 2 112 cm^{-1} emerges at higher CO exposure. The former one is assigned to atop CO on Pd and the latter one to atop CO on Au. Over the entire exposure range, no feature related to CO on bridging or tri-hollow sites of Pd is evident. These results confirm the formation of surface isolated Pd monomers after annealing at 800 K.

2.3 The origin of the promotional effects of Au

The above LEIS and CO-IRAS results demonstrate the formation of exclusively monomeric Pd sites at low surface Pd coverage both on Pd/Au single crystal and on Pd-Au bimetal thin films on Mo(110). This confirms that the higher VA formation rate observed at lower Pd coverages for Pd/Au is indeed due to the increased fraction of surface Pd monomers. Then why is the catalytic performance for a surface with Pd monomers superior to one with contiguous Pd atoms? In the following, CO-TPD and C_2H_4-TPD were used to probe properties of these two surfaces, since CO is one of the reaction intermediates or by-products and C_2H_4 is one of the reactants.

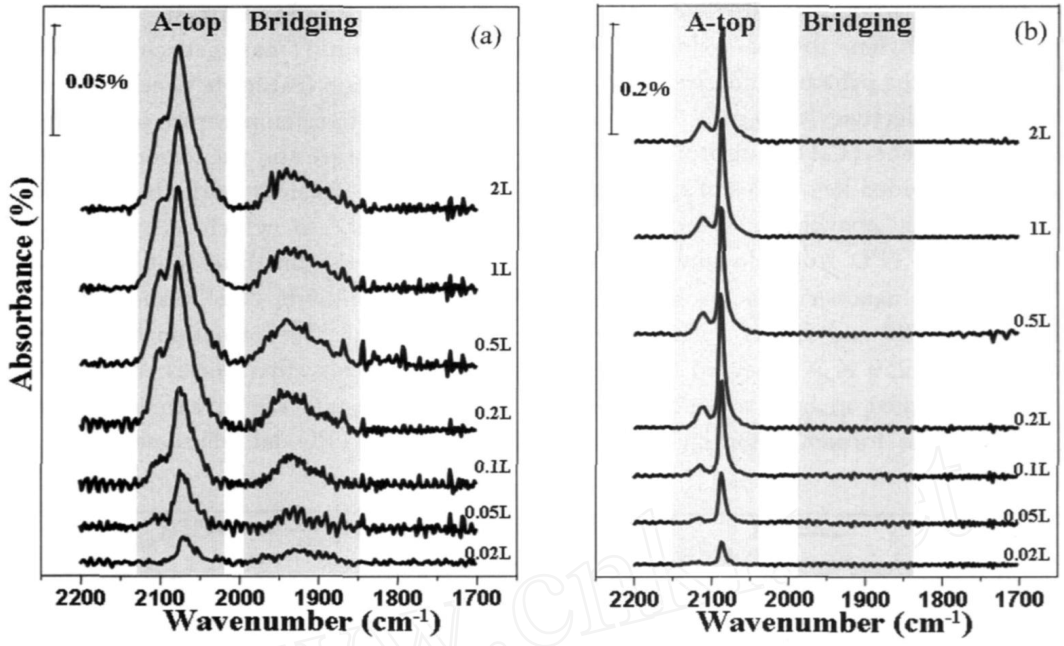

Fig 5　IRAS of CO on 5 ML Pd/ 5 ML Au/ Mo(110) annealed for 20 min at different temperature as a function of CO exposure[35]
(a) 600 K, (b) 800 K

The thermal behavior of CO on the Pd-Au alloy surface was compared with that on a Pd surface using TPD as shown in Fig 6[35]. CO-TPD from a 5 ML Pd/ 5 ML Au/ Mo(110) annealed at 800 K shows a main feature at ~300 K (see Fig 6(a)). Features at ~450 K for low CO coverages and between 300-450 K for saturated CO coverage were observed for multilayer Pd on Mo(110) surface (see Fig 6(b)), consistent with previous observations on Pd(111)[35,52]. Such significant differences between Pd-Au alloy surfaces and Pd surfaces is consistent with the formation of isolated Pd monomers on the alloy surface, as confirmed by LEIS and CO-IRAS[35]. The much lower desorption temperature of ~300 K for CO on Pd monomer sites compared to ~450 K for CO on contiguous Pd is significant considering that the VA synthesis reaction temperature lies generally between 393-453 K. As mentioned above, CO is a reaction by-product. The higher desorption temperature on contiguous Pd sites may result in poisoning of surface

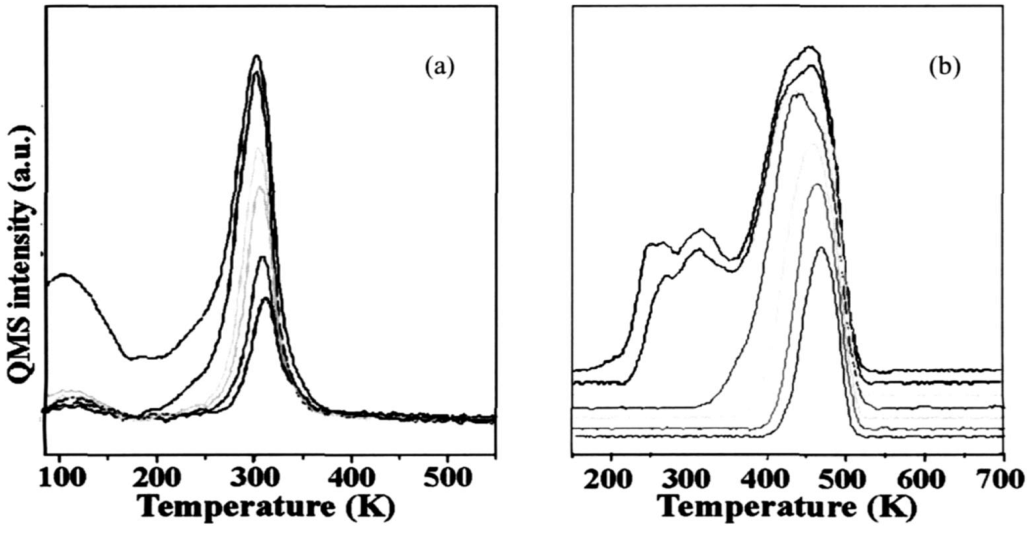

Fig 6　TPD of CO on 5 ML Pd/ 5 ML Au/ Mo(110) (a) and 10 ML Pd/ Mo(110) (b) annealed at 800 K for 20 min with various CO exposure (0.01-0.5 L)[35]

active sites by CO, leading to lower catalytic activity of these sites compared to isolated Pd sites.

In acetoxylation of ethylene to VA, oxidation of ethylene to CO_x is one of the primary undesirable side reactions, lowering the selectivity toward VA. TPD studies of deuterated ethylene (C_2D_4) adsorption and dehydrogenation have provided key pieces of information regarding the catalytic conversion of ethylene. Fig 7 (a) compares C_2D_4-TPD from Pd and Pd-Au nanoparticles[34]. For Pd nanoparticles on silica, a desorption peak between 180 and 330 K with a peak desorption temperature of 250 K is observed. Such a broad feature can be assigned to both π-bonded and di-σ-bonded C_2D_4 with the former desorbing at the lower temperature and the latter, at the higher temperature[2,54-56]. In contrast, C_2D_4-TPD on Pd-Au (1∶1 atomic ratio) nanoparticles shows a much narrower desorption feature between 180 and 260 K with a peak desorption temperature of 215 K. The sharper desorption feature and the lower peak desorption temperature are consistent with the formation of isolated Pd monomers, to which ethylene can π-bond[2]. These results demonstrate that the addition of Au to Pd clusters inhibits the formation of adjacent Pd atoms and thus the formation of the strongly bound di-σ-C_2D_4 species, the species that converts to ethylidyne. The results are in agreement with the CO-IRAS and CO-TPD data discussed above.

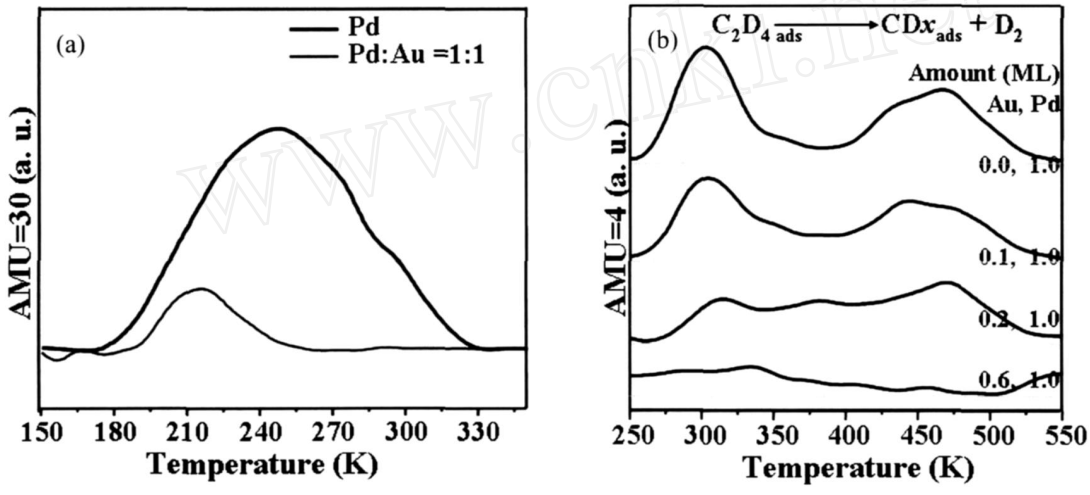

Fig 7 (a) TPD of C_2D_4 with 2.0 L C_2D_4 exposure at 85 K on 1 ML Pd/SiO_2 and 1 ML Au/1 ML Pd/SiO_2[34]; (b) D_2 signals collected from C_2D_4 TPD with 2.0 L C_2D_4 exposure at 85 K on Pd/SiO_2 and Au-Pd/SiO_2 surfaces[34]

Pd has been reported to catalyze ethylene decomposition on Pd(111), Pd(100) and alumina supported Pd cluster surfaces[54-56]. Ethylene decomposition is believed to be promoted by a strong interaction between ethylene and two adjacent Pd atoms. Ethylidyne (≡CCH_3) and vinyl (-CH-CH_2) species are proposed to be the reaction intermediates on Pd(111) and Pd(100) facets, respectively, with the reaction site requiring three-fold hollow and bridging Pd sites. Thus, D_2-TPD during ethylene desorption is useful to monitor the ethylene decomposition. Fig 7(b) shows D_2 formation during C_2D_4-TPD on silica-supported Pd and Pd-Au nanoparticles. For C_2D_4 dehydrogenation on Pd nanoparticles, two D_2 features appear with desorption peak maxima at 310 and 470 K. With the addition of 0.1, 0.2 and 0.4 ML of Au to 1.0 ML Pd/SiO_2 and a subsequent anneal at 800 K, the production of D_2 from C_2D_4 TPD gradually decreases. With the addition of 0.6 ML Au, the D_2 production becomes negligible. Such results clearly demonstrate that contiguous Pd sites are required for ethylene decomposition. The lack of suitable surface adsorption sites, i.e., three-fold hollow and bridging Pd sites, in Pd-Au alloy surfaces accounts for the suppression of D_2 production. It is obvious that the formation of isolated Pd surface monomers also inhibits ethylene decomposition and thus enhances the selectivity and activity for VA synthesis.

3 Conclusions

From model catalytic systems of Pd/Au(100) and Pd(111), we have found that isolated Pd monomer surface sites are more active for acetoxylation of ethylene to VA compared to contiguous Pd surface sites. The main role of Au is to isolate Pd monomer sites. The origin of the promotional effects

of Au can thus be attributed to the following two points. First, the bonding strength of CO on Pd monomer sites is much weaker than that on contiguous Pd sites, thus reducing the poisoning effect of CO. Second, contiguous Pd sites, though active for VA synthesis, are also active for ethylene decomposition and combustion to CO_x and H_2O. By forming surface isolated Pd monomers, the path of ethylene decomposition is blocked due to absence of Pd bridging and/or tri-hollow sites. As a consequence, higher selectivities and activities for VA formation can be achieved on Au promoted Pd catalysts.

Acknowledgments

We acknowledge with pleasure the financial support of this work by Department of Energy, Office of Basic Energy, Division of Chemical Sciences, and Robert A Welch Foundation.

References

1 Rodriguez J A, Goodman D W. *Science*, 1992, **257**(5072): 897
2 Chen M S, Luo K, Wei T, Yan Z, Kumar D, Yi C W, Goodman D W. *Catal Today*, 2006, **117**(1-3): 37
3 Chen M S, Kumar D, Yi C W, Goodman D W. *Science*, 2005, **310**(5746): 291
4 Rodriguez J A, Jirsak T, Chaturvedi S, Hrbek J. *J Am Chem Soc*, 1998, **120**(43): 11149
5 Besenbacher F, Chorkendorff I, Clausen B S, Hammer B, Molenbroek A M, Norskov J K, Stensgaard I. *Science*, 1998, **279**(5358): 1913
6 Allison E G, Bond G C. *Catal Rev Sci Eng*, 1972, **7**(2): 233
7 Rylander P N. Catalytic Hydrogenation in Organic Synthesis. London: Academic Press, 1979
8 Abel R, Collins P, Eichler K, Nicolau I, Peters D. In: Ertl G, Knözinger H, Weitkamp J eds. Handbook of Heterogeneous Catalysis. Vol 5. Weinheim: Wiley VCH, 1997. 2298
9 Venezia A M, La Parola V, Nicoli V, Deganello G. *J Catal*, 2002, **212**(1): 56
10 Trimm D L, Onsan Z I. *Catal Rev*, 2001, **43**(1-2): 31
11 Bonarowska M, Malinowski A, Juszczyk W, Karpinski Z. *Appl Catal B*, 2001, **30**(1-2): 187
12 Menegazzo F, Burti P, Signoretto M, Manzoli M, Vankova S, Boccuzzi F, Pinna F, Strukul G. *J Catal*, 2008, **257**(2): 369
13 Pluntke Y, Kibler L A, Kolb D M. *Phys Chem Chem Phys*, 2008, **10**(25): 3684
14 Hutchings G J. *Chem Commun*, 2008, (10): 1148
15 Wang D, Villa A, Porta F, Prati L, Su D S. *J Phys Chem C*, 2008, **112**(23): 8617
16 Knecht M R, Weir M G, Frenkel A I, Crooks R M. *Chem Mater*, 2008, **20**(3): 1019
17 Teng X W, Wang Q, Liu P, Han W, Frenkel A, Wen W, Marinkovic N, Hanson J C, Rodriguez J A. *J Am Chem Soc*, 2008, **130**(3): 1093
18 Fan F R, Liu D Y, Wu Y F, Duan S, Xie Z X, Jiang Z Y, Tian Z Q. *J Am Chem Soc*, 2008, **130**(22): 6949
19 Ma C Y, Li X H, Jin M S, Liao W P, Guan R G, Suo Z H. *Chin J Catal*, 2007, **28**(6): 535
20 Han Y F, Zhong Z Y, Ramesh K, Chen F X, Chen L W, White T, Tay Q L, Yaakub S N, Wang Z. *J Phys Chem C*, 2007, **111**(24): 8410
21 Piednoir A, Languille M A, Piccolo L, Valcarcel A, Aires F J C S, Bertolini J C. *Catal Lett*, 2007, **114**: 110
22 Nutt M O, Heck K N, Alvarez P, Wong M S. *Appl Catal B*, 2006, **69**(1-2): 115
23 Ma Z, Zaera F. *Surf Sci Rep*, 2006, **61**(5): 229
24 Nakamura S, Yasui T. *J Catal*, 1970, **17**(3): 366
25 Samanos B, Boutry P. *J Catal*, 1971, **23**(1): 19
26 Provine W D, Mills P L, Lerou J J. *Stud Surf Sci Catal*, 1996, **101**: 191
27 Macleod N, Keel J M, Lambert R M. *Appl Catal A*, 2004, **261**(1): 37
28 Han Y F, Kumar D, Goodman D W. *J Catal*, 2005, **230**(2): 353
29 Han Y F, Wang J H, D. Kumar D, Yan Z, Goodman D W. *J Catal*, 2005, **232**(2): 467
30 Kumar D, Han Y F, Chen M S, Goodman D W. *Catal Lett*, 2006, **106**(1-2): 1
31 Kumar D, Chen M S, Goodman D W. *Catal Today*, 2007, **123**(1-4): 77
32 Stacchiola D, Calaza F, Burkholder L, Tysoe W T. *J Am Chem Soc*, 2004, **126**(47): 15384
33 Neurock M, *J Catal*, 2003, **216**(1-2), 73
34 Luo K, Wei T, Yi C W, Axnanda S, Goodman D W. *J Phys Chem B*, 2005, **109**(49): 23517
35 Yi C W, Luo K, Wei T, Goodman D W. *J Phys Chem B*, 2005, **109**: 18535
36 Wei T, Kumar D, Chen M S, Luo K, Axnanda S, Lundwall M, Goodman D W. *J Phys Chem C*, 2008, **112**(22): 8332
37 Chen M S, Santra A K, Goodman D W. *Phys Rev B*, 2004, **69**(15): 155404
38 Chen M S, Goodman D W. *Surf Sci*, 2006, **600**(19): L255
39 Chen M S, Goodman D W. *Science*, 2004, **306**(5694): 252
40 Kuhn W K, Szanyi J, Goodman D W. *Surf Sci*, 1992, **274**(3): L611
41 Campbell C T. *Current Opinion Solid State Mater Sci*, 1998, **3**(5): 439
42 Wolter K, Seiferth O, Libuda J, Kuhlenbeck H, Baumer M, Freund H J. *Surf Sci*, 1998, **404**(1-3): 428
43 Koel B E, Sellidj A, Paffett M T. *Phys Rev B*, 1992, **46**(12): 7846
44 Baddeley C J, Barnes C J, Wander A, Ormerod R M, King D A, Lambert R M, *Surf Sci*, 1994, **314**(1): 1
45 Maroun F, Ozanam F, Magnussen O M, Behm R J, *Sci-*

ence, 2001, **293**(5536): 1811
46 Han P, Axnanda S, Lyubinetsky I, Goodman D W. *J Am Chem Soc*, 2007, **129**(46): 14355
47 Anton R, Eggers H, Veletas J. *Thin Solid Films*, 1993, **226**(1): 39
48 Mezey L Z, Giber J. *Jpn J Appl Phys*, 1982, **21**: 1569
49 Li Z J, Furlong O, Calaza F, Burkholder H C, Poon D, Saldin D, Tysoe W T. *Surf Sci*, 2008, **602**(5): 1084
50 Soto-Verdugo V, Metiu H. *Surf Sci*, 2007, **601**(23): 5332
51 Yuan D W, Gong X G, Wu R Q. *Phys Rev B*, 2007, **75**(23): 233401
52 Guo X C, Yates J T. *J Chem Phys*, 1989, **90**(11): 6761
53 Ozensoy E, Goodman D W. *Phys Chem Chem Phys*, 2004, **6**(14): 3765
54 Guo X, Madix R J. *J Am Chem Soc*, 1995, **117**(20): 5523
55 Shaikhutdinov Sh, Heemeier M, Baumer M, Lear T, Lennon D, Oldman R J, Jackson S D, Freund H J. *J Catal*, 2001, **200**(2): 330
56 Stuve E M, Madix R J. *Surf Sci*, 1985, **160**(1): 293